

Understanding kinematics of ν_μ - CC interaction using MINERvA experiment

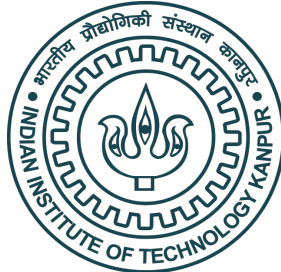
*A Thesis Submitted
in Partial Fulfilment of the Requirements
for the Degree of*

INTEGRATED MASTER OF SCIENCE in Physics

by

**N Gokul
(Reg. No. 35218045)**

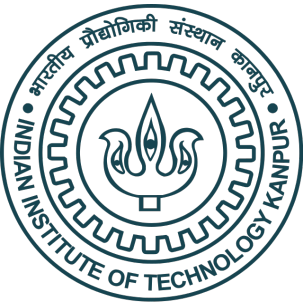
Under the guidance of



**Prof. Navaneeth Poonthottathil
Department of Physics
Indian Institute of Technology Kanpur**



**Centre for Integrated Studies
Cochin University of Science and Technology**



Department of Physics
Indian Institute of Technology
Kanpur

Certificate

This is to certify that the project report titled "**Understanding kinematics of ν_μ - CC interaction using MINERvA experiment**" is bona fide work done by **N Gokul** (Reg no 35218045), in the Department of Physics, **Indian Institute of Technology**, under the guidance of **Dr Navaneeth Poonthottathil**, Assistant Professor for the partial fulfilment of the requirements for the award of the degree of Integrated Master of Science in Physics from Cochin University of Science and Technology.



Prof. Dr. Navaneeth Poonthottathil

Project Supervisor

Assistant Professor

Department of Physics

IIT Kanpur



Department of Physics
Cochin University of Science and Technology
Kochi

Certificate

This is to certify that the project report titled "**Understanding kinematics of ν_μ - CC interaction using MINERvA experiment**" is the bona fide work done by N Gokul (Reg no 35218045), in the Department of Physics, Indian Institute of Technology, under the guidance of Dr Navaneeth Poonthotathil, Assistant Professor for the partial fulfilment of the requirements for the award of the degree of Master of Science in Physics from Cochin University of Science and Technology..



Dr Titus K Mathew

Professor

Internal Faculty In-Charge for MSc Project

Head of the Department

Department of Physics

CUSAT



PROFESSOR & HEAD
Department of Physics
Cochin University of
Science and Technology
Kochi - 682 022, Kerala

DECLARATION

I hereby declare that the work presented in this thesis titled “**Understanding kinematics of ν_μ - CC interaction using MINERvA experiment**” is based on the original work done by me under the guidance of Dr Navaneeth Poonthottathil, Assistant Professor, Indian Institute of Technology Kanpur.

Kochi - 682 022

N Gokul

June 2023

ACKNOWLEDGEMENT

I express my deep gratitude to my mentor and supervisor Prof. Navaneeth Poonthottathil of IIT, Kanpur for hosting me and providing constant support and motivation throughout the project.

I would like to extend my sincere gratitude to my Internal supervisor for the MSc project and the Head of the department Dr. Titus K Mathew. I am indebted to my mentor Dr. Senoy Thomas for the support throughout the course. I am grateful to my course co-ordinator Dr Sasidevan. I like to express my gratitude to all the faculties. I would like to acknowledge Minerva group for the easily accessible dataset.

I would like to convey my heartfelt appreciation to all my friends and my parents for their unconditional love and support.

I acknowledge Overleaf, an online L^AT_EX editor and collaboration platform, for providing a user-friendly and efficient environment for writing and editing my thesis.

Lastly, I would like to express my sincere obligation towards all, whose names I might have left out, who have extended their support and well wishes for me.

N Gokul

ABSTRACT

The main aim of the project is to find the energy of (muon)neutrino from CCQE interaction using muon kinematics. For this study, data from MINERvA is used and macros coded in Root-framework is used for analysis. Plots of muon and proton momentum are made and energy is calculated using muon kinematics. Plots of neutrino energy are made and fit with gaussian curve.

Keywords: CCQE, neutrino interaction, Muon-neutrino, energy estimation, charged-current quasi-elastic.

Contents

List of Figures	viii
1 Introduction	1
1.1 Neutrino	2
1.1.1 Solar Neutrino Deficit	2
1.1.2 Neutrino Oscillation	4
2 Neutrino Physics	5
2.1 Weyl, Dirac and Majorana neutrinos	5
2.2 Neutrino oscillation	7
2.3 Neutrino oscillation in vacuum: Two-flavour	8
2.4 Neutrino oscillation in vacuum: Three-flavour	12
2.5 Matter Effect	16

2.6	Neutrino Mass Hierarchy: Inverted and Normal ordering	16
2.7	Neutrino Interaction	17
3	MINERvA	22
3.1	Introduction	22
3.2	NuMI	23
3.3	Nuclear Targets and Detector	25
3.4	Calorimetry and Minos	28
3.4.1	Calorimetry	28
3.4.2	Minos	29
3.5	Resolution	29
3.6	Arachne	30
3.6.1	Arachne-display	30
4	Results and Discussions	32
4.1	Momentum	33
4.1.1	Muon - Momentum	33
4.1.2	proton - Momentum	34

4.1.3	Muon-neutrino - Momentum	34
4.2	Reconstructed Energy	36
4.3	de Broglie wavelength	37
4.4	Caveats in analysis	38
5	Conclusion	40
Appendices		42
A	Dirac Equation	42
A.1	Dirac Equation	42
A.2	Weyl equation	44
B	Matter Effect	46
B.1	Hamiltonian for neutrino in vacuum	47
B.2	Matter Hamiltonian	49
C	Additional Context	51
C.1	Systematic errors	51
C.2	ROOT	52
Bibliography		53

List of Figures

1.1	Neutrino Interaction	2
1.2	Different steps in the fusion reaction and neutrino production in the Sun. (all ν are ν_e)[1]	3
1.3	Visualisation of neutrino oscillation	4
2.1	Neutrino[8]	6
2.2	Different oscillations of neutrinos	15
2.3	Normal Inverted Mass ordering[14]	17
2.4	Cross section of different interaction of muon-neutrino[16]	19
2.5	Different neutrino interaction. The time axis is vertical in all figures .	20
3.1	Different accelerators[18]	23
3.2	NuMI:Neutrino production(neutrino mode)[19]	24

3.3	Minerva Nuclear targets	25
3.4	Triangular Plastic scintillator[Right], with WLS fibre[Left][20]	26
3.5	PMT[20]	26
3.6	X, U and V planes	27
3.7	Minerva. Right: Cross-sectional view. Left: Longitudinal view showing different components[20]	27
3.8	Differential identification of particles[22]	28
3.9	Minerva event display samples(All images taken from Minerva Website)	31
4.1	Distribution of Muon momentum. All plots are integral normalised.	33
4.2	Distribution of proton momentum. All plots are integral normalised.	34
4.3	Distribution of ν_μ momentum. All plots are integral normalised. . .	35
4.4	Reconstructed Energy of ν_μ by (a) QE energy reconstruction; (b) sum of kinetic energies of products	37
4.5	de Broglie wavelength of μ -neutrinos($1 \text{ fm} = 10^{-15} \text{ m}$)	38

Chapter 1

Introduction

The terminologies in particle physics are often confusing. With the standard model, we can classify particles as bosons, leptons and quarks. Leptons and quarks are fermions with half-integer spin values. Quarks have colour and come in six flavours in three generations. Lepton contains six flavours and three generations and has no colour. The three generations are in increasing order of masses considering the charged leptons.

Table 1.1: Leptons

Gen 1	Gen 2	Gen 3
$\begin{pmatrix} e \\ \nu_e \end{pmatrix}$	$\begin{pmatrix} \mu \\ \nu_\mu \end{pmatrix}$	$\begin{pmatrix} \tau \\ \nu_\tau \end{pmatrix}$

1.1 Neutrino

The neutrinos are chargeless leptons which interact only via the weak force. The force carriers of weak interaction are W^\pm and Z boson.

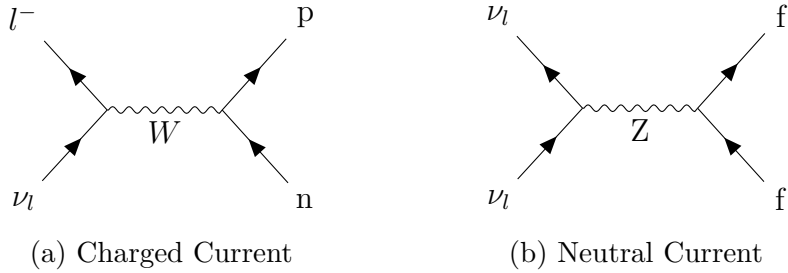


Figure 1.1: Neutrino Interaction

The charged-current interaction (1.1a) can assign flavours to the neutrino. If the lepton, l^- , is observed to be an electron, then the neutrino is electron-neutrino(ν_e). Similarly, if l^- is μ^- then the neutrino is muon-neutrino (ν_μ), and is tau-neutrino (ν_τ) if l^- is τ^- .

1.1.1 Solar Neutrino Deficit

Through the pp-cycle, the Sun produces electron-neutrinos at various stages. Figure 1.2 shows the different reactions and their percentage rates.

In 1965, at Homestake Mine, a chlorine-based neutrino detector was proposed by Dr Ray Davis Jr. This experiment was intended to study the solar neutrino flux. The chemical used was liquid tetracholoro-ethylene. The detector used the reaction $^{37}\text{Cl} + \nu_e \rightarrow ^{37}\text{Ar} + e^-$ or ($^{37}\text{Cl}(\nu_e, e^-)^{37}\text{Ar}$ in short notation).

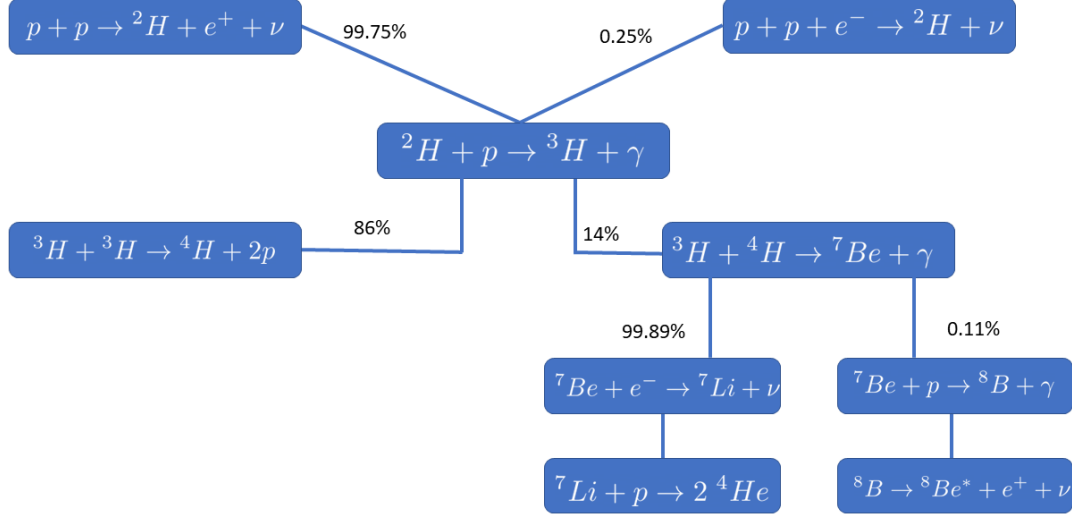


Figure 1.2: Different steps in the fusion reaction and neutrino production in the Sun. (all ν are ν_e)[1]

In 1968, Davis and collaborators announced the upper bound on solar neutrino flux as 3 SNU¹²[2]. At the same time, accompanying this paper was the published work of Bahcall, Bahcall and Shaviv[3], who calculated the flux of solar neutrino theoretically. They found the flux to be 7.5 ± 0.3 SNU. The detected flux was less than one-third of the theoretical value. This discrepancy is huge even if we consider all experimental errors.

¹SNU: solar neutrino unit

²1 SNU = 10^{-36} captures per target atom per second

1.1.2 Neutrino Oscillation

The concept of neutrino oscillation was proposed in 1967 by Pontecorvo[4]. The idea proposed by Pontecorvo is that the neutrino can oscillate between different flavours as they travel through a vacuum. This oscillation depends on its energy and the distance travelled. This implies that the electron-neutrino from solar nuclear activity changed flavours while travelling through the vacuum. This formulation solves the solar neutrino deficit problem as the chlorine detector was sensitive only to the electron-neutrinos. The oscillation is explained via the mixing of flavour states $\{ \nu_e, \nu_\mu, \nu_\tau \}$ and the mass eigenstates $\{ \nu_1, \nu_2, \nu_3 \}$

For simplicity, the two flavour mixing can be visualised as shown in figure 1.3; however, this visualisation is not the right way. The formulation is explained in Chapter 2.

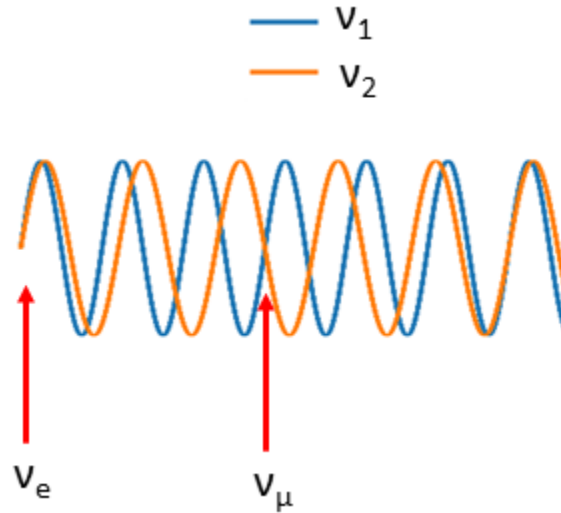


Figure 1.3: Visualisation of neutrino oscillation

Chapter 2

Neutrino Physics

2.1 Weyl, Dirac and Majorana neutrinos

Weyl

Neutrinos, if treated as massless particles, will allow us to decouple the Dirac equation¹. All neutrinos are left-handed, and anti-neutrinos are right-handed in any frame of reference. This is because mass-zero particles travel at the speed of light, and it is impossible to find a frame of reference faster than the speed of light. Therefore, neutrinos and anti-neutrinos are two particles with opposite lepton numbers and definite helicity[5], i.e. anti-neutrinos will always be right-handed, and neutrinos will always be left-handed.

¹Appendix A.2

Dirac

If the neutrinos have mass, they will travel at a speed less than the speed of light. Hence we could formulate a frame of reference faster than the speed of neutrino. This implies that a left-handed neutrino, Ψ_L^ν will become right-handed, Ψ_R^ν at a boosted frame and right-handed anti-neutrino, $\bar{\Psi}_R^{\bar{\nu}}$ will appear left-handed, $\bar{\Psi}_L^{\bar{\nu}}$ ². Therefore we will have four spinors, Ψ_L^ν , Ψ_R^ν , $\bar{\Psi}_R^{\bar{\nu}}$, $\bar{\Psi}_L^{\bar{\nu}}$. If we assume $\Psi_R^{\bar{\nu}}$ is not the same as $\bar{\Psi}_R^{\bar{\nu}}$, then we could say that $\Psi_L^{\bar{\nu}}$ has a CPT image $\bar{\Psi}_L^{\bar{\nu}}$. Such four states with the same mass exist and are called Dirac neutrinos[6].

Majorana

In 1937, Majorana introduced the concept of a particle and its antiparticle being identical[7]. If neutrinos are Majorana particles, the particle obtained by applying the Lorentz transformation will be the same as that obtained by applying CPT. Both will result in Ψ_R^ν if we initially consider Ψ_L^ν . Here there are two states with the same masses. $\Psi_R = \bar{\Psi}_R$, and $\Psi_L = \bar{\Psi}_L$. These are called majorana neutrinos.

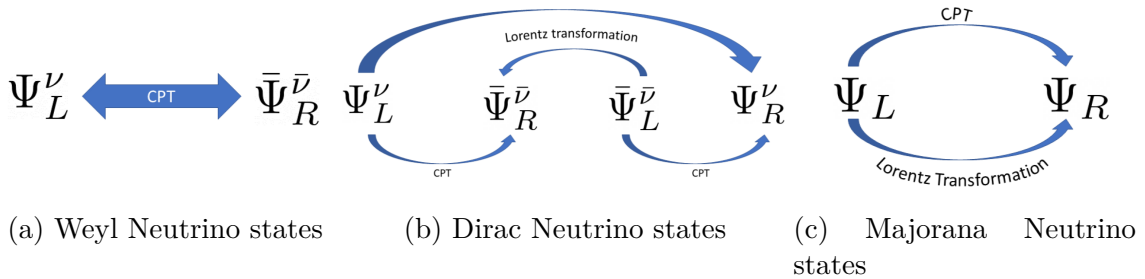


Figure 2.1: Neutrino[8]

²Lorentz transformation will not change the spin of the particle

2.2 Neutrino oscillation

The mixing of flavour state with mass eigenstate is a quantum mechanical phenomenon. Each of the flavour states $|\nu_\alpha\rangle$ can be written as a superposition of mass eigen state denoted as $|\nu_i\rangle$, where $\alpha \in \{e, \mu, \tau\}$ and $i \in \{1, 2, 3\}$.

$$|\nu_\alpha\rangle = \sum_{i=1}^3 U_{\alpha i} |\nu_i\rangle \quad (2.1)$$

We can write the same equation in matrix form as

$$\begin{pmatrix} \nu_e \\ \nu_\mu \\ \nu_\tau \end{pmatrix} = \begin{pmatrix} U_{e1} & U_{e2} & U_{e3} \\ U_{\mu 1} & U_{\mu 2} & U_{\mu 3} \\ U_{\tau 1} & U_{\tau 2} & U_{\tau 3} \end{pmatrix} \begin{pmatrix} \nu_1 \\ \nu_2 \\ \nu_3 \end{pmatrix} \quad (2.2)$$

The U matrix is called PMNS³ matrix. The standard parametrization is inspired by the CKM⁴ matrix, which gives the mixing in the quark sector. We require the U matrix to be unitary, i.e. $UU^\dagger = 1$. In general, for a model of n neutrinos, the parameterisation of the PMNS matrix with Euler angles will require $\frac{n(n-1)}{2}$ angles and $\frac{n(n-2)}{2}$ CP phases. For the current model of $n = 3$, there are 3 angles θ and if we consider Dirac, one CP phase δ_{CP} [9], for Majorana neutrinos, the number of phases will be $\frac{n(n-1)}{2} = 3$ [10]. The standard parametrisation of the matrix is

³Pontecorvo-Maki-Nagakawa-Sakata

⁴Cabbibo-Kobayashi-Maskawa

$$U = \begin{pmatrix} c_{12} & s_{12} & 0 \\ -s_{12} & c_{12} & 0 \\ 0 & 0 & 1 \end{pmatrix} \begin{pmatrix} c_{13} & 0 & s_{13}e^{-i\delta_{CP}} \\ 0 & 1 & 0 \\ s_{13}e^{i\delta_{CP}} & 0 & c_{13} \end{pmatrix} \begin{pmatrix} 1 & 0 & 0 \\ 0 & c_{23} & s_{23} \\ 0 & -s_{23} & c_{23} \end{pmatrix} P \quad (2.3)$$

Where $c_{ij} = \cos\theta_{ij}$ and $s_{ij} = \sin\theta_{ij}$. δ_{cp} is often called Dirac's phase, which represents CP- violation. P is a matrix containing Majorana phases which do not contribute to oscillation. This matrix has several different parameterisations and is significant in events like neutrino-less double β -decay.

2.3 Neutrino oscillation in vacuum: Two-flavour

Let us consider any two flavours(let them be μ and e) of neutrino and two mass eigenstates, say ν_1 and ν_2 . Then the mixing of mass eigenstates in the flavour state can be expressed as,

$$|\nu_\alpha\rangle = \sum_{i=1}^2 U_{\alpha i} |\nu_i\rangle \quad (2.4)$$

In matrix form,

$$\begin{pmatrix} \nu_e \\ \nu_\mu \end{pmatrix} = \begin{pmatrix} U_{e1} & U_{e2} \\ U_{\mu 1} & U_{\mu 2} \end{pmatrix} \begin{pmatrix} \nu_1 \\ \nu_2 \end{pmatrix} \quad (2.5)$$

We can also express the mixing of flavour states in mass eigenstate as,

$$|\nu_i\rangle = \sum_\alpha U_{\alpha i}^* |\nu_\alpha\rangle \quad (2.6)$$

We require the matrix U to satisfy the conditions,

$$UU^\dagger = 1 \quad (2.7)$$

$$\sum_{\alpha} U_{\alpha i} U_{\alpha j}^* = \delta_{ij} \quad \text{and} \quad \sum_i U_{\alpha i} U_{\beta i}^* = \delta_{\alpha\beta} \quad (2.8)$$

U is a 2×2 unitary matrix with real entries. We can parametrise the matrix and rewrite mixing as

$$\begin{pmatrix} \nu_e \\ \nu_\mu \end{pmatrix} = \begin{pmatrix} \cos \theta & \sin \theta \\ -\sin \theta & \cos \theta \end{pmatrix} \begin{pmatrix} \nu_1 \\ \nu_2 \end{pmatrix} \quad (2.9)$$

Here we call θ as the mixing angle. The sum of the probability of survival of a flavour and changing into another flavour should be 1. Therefore,

$$P(\nu_e \rightarrow \nu_e) + P(\nu_e \rightarrow \nu_\mu) = P(\nu_\mu \rightarrow \nu_\mu) + P(\nu_\mu \rightarrow \nu_e) = 1 \quad (2.10)$$

To find the formula for probability, we should consider the time evolution of the flavour state. We can start with the Schrödinger equation

$$i \frac{\partial |\nu_\alpha(t)\rangle}{\partial t} = H |\nu_\alpha(t)\rangle \quad (2.11)$$

H is the Hamiltonian. If $|\nu_\alpha(0)\rangle$ denotes the state of flavour state at time $t=0$, then the Schrödinger equation 2.11 can be solved as

$$|\nu_\alpha(t)\rangle = e^{-iHt} |\nu_\alpha(0)\rangle = e^{-iEt} |\nu_\alpha(0)\rangle \quad (2.12)$$

For mass eigenstates,

$$H |\nu_i\rangle = E_i |\nu_i\rangle \quad i = 1, 2 \quad (2.13)$$

Therefore, we can write equation 2.12 as

$$|\nu_\alpha(t)\rangle = \sum_{i=1}^2 e^{-iE_i t} U_{\alpha i} |\nu_i\rangle \quad (2.14)$$

For computing the probability of initially β flavour to change to α , we can find $\langle \nu_\beta(0) | \nu_\alpha(t) \rangle$, which is called amplitude, and take its square.

$$\begin{aligned} \langle \nu_\beta(0) | \nu_\alpha(t) \rangle &= \sum_{j=1}^2 U_{\beta j}^* \langle \nu_j | \sum_{i=1}^2 e^{-iE_i t} U_{\alpha i} |\nu_i\rangle \\ &= \sum_{j=1}^2 \sum_{i=1}^2 e^{-iE_i t} U_{\beta j}^* U_{\alpha i} \langle \nu_j | \nu_i \rangle \\ &= \sum_{i=1}^2 e^{-iE_i t} U_{\beta i}^* U_{\alpha i} \end{aligned} \quad (2.15)$$

$$\begin{aligned} P(\nu_\beta \rightarrow \nu_\alpha) &= |\langle \nu_\beta(0) | \nu_\alpha(t) \rangle|^2 \\ &= (\sum_{i=1}^2 e^{-iE_i t} U_{\beta i}^* U_{\alpha i}) (\sum_{j=1}^2 e^{-iE_j t} U_{\beta j}^* U_{\alpha j})^* \\ &= \sum_{i=1}^2 \sum_{j=1}^2 e^{-i(E_i - E_j)t} U_{\beta i}^* U_{\alpha i} U_{\beta j} U_{\alpha j}^* \end{aligned} \quad (2.16)$$

Using the approximation, $E_1 \approx E_2 \approx p \approx E$

$$E_i - E_j = \frac{E_i^2 - E_j^2}{E_i + E_j} \approx \frac{m_i^2 - m_j^2}{E_i + E_j} \approx \frac{\Delta m_{ij}^2}{2E}$$

Expanding the equation 2.16, for $\alpha \rightarrow \beta$, we get,

$$\begin{aligned}
P(\nu_\alpha \rightarrow \nu_\beta) &= |U_{\beta 1}|^2 |U_{\alpha 1}|^2 + |U_{\beta 2}|^2 |U_{\alpha 2}|^2 + e^{-i(E_1 - E_2)t} U_{\beta 1}^* U_{\alpha 1} U_{\beta 2} U_{\alpha 2}^* + e^{-i(E_2 - E_1)t} U_{\beta 2}^* U_{\alpha 2} U_{\beta 1} U_{\alpha 1}^* \\
&= \sin^2 \theta \cos^2 \theta + \sin^2 \theta \cos^2 \theta + 2(\cos \theta)(-\sin \theta)(\sin \theta)(\cos \theta) \cos(E_2 - E_1)t \\
&= 2 \sin^2 \theta \cos^2 \theta - 2 \cos^2 \theta \sin^2 \theta \cos(E_2 - E_1)t \\
&= 2 \sin^2 \theta \cos^2 \theta (1 - \cos \frac{\Delta m^2}{2E} t) \\
&= \sin^2 2\theta \sin^2 (\frac{\Delta m^2}{4E} t) \tag{2.17}
\end{aligned}$$

$$= \sin^2 2\theta \sin^2 (\Delta m^2 \frac{L}{4E}) \tag{2.18}$$

$$= \sin^2 2\theta \sin^2 (1.267 \Delta m^2 \frac{L}{E}) \tag{2.19}$$

In equation 2.17, we have substituted $t = L$ to obtain equation 2.18. Up to this point, we have assumed $\hbar = c = 1$. In equation 2.19, we have rewritten such that the units of L is in km, Δm is in eV and E is in GeV. For survival probability, $\alpha \rightarrow \alpha$, can use

$$\begin{aligned}
P(\nu_\alpha \rightarrow \nu_\alpha) &= 1 - P(\nu_\alpha \rightarrow \nu_\beta) \\
&= 1 - \sin^2 2\theta \sin^2 (1.267 \Delta m^2 \frac{L}{E}) \tag{2.20}
\end{aligned}$$

Let $L^{osc} = 2.48 \frac{E}{\Delta m^2}$. L^{osc} is called the oscillation length. when,

1. $L \ll L^{osc}$, there are no oscillation
2. $L \gg L^{osc}$, the oscillations are averaged out

This leads to the condition for detecting the oscillation

$$\Delta m^2 \frac{L}{E} \approx 1$$

2.4 Neutrino oscillation in vacuum: Three-flavour

We can find the probability for three-flavour in a similar way. We can start using the mixing form shown in 2.1 and 2.2 using the parameterisation used in 2.3. Here we will not worry about P.

Following the same procedure we did for two flavour case, we can write the oscillation probability for $\alpha \rightarrow \beta$ as

$$P(\alpha \rightarrow \beta) = \sum_{i,j=1}^3 U_{\alpha i} U_{\beta i}^* U_{\alpha j}^* U_{\beta j} e^{\frac{L}{2E} \Delta m_{ji}^2}$$

Decomposing the summation into convenient pieces, we will arrive at,

$$\begin{aligned} P(\alpha \rightarrow \beta) &= \sum_{i=j} U_{\alpha i}^* U_{\beta i} U_{\alpha j} U_{\beta j}^* + \sum_{i \neq j} U_{\alpha i}^* U_{\beta i} U_{\alpha j} U_{\beta j}^* - 2 \sum_{i \neq j} U_{\alpha i}^* U_{\beta i} U_{\alpha j} U_{\beta j}^* \sin^2 \left(\frac{L}{4E} \Delta m_{ji}^2 \right) \\ &\quad + \iota \sum_{i \neq j} U_{\alpha i}^* U_{\beta i} U_{\alpha j} U_{\beta j}^* \sin \left(\frac{L}{2E} \Delta m_{ji}^2 \right) \end{aligned}$$

We can call the first term P_1 , the second term P_2 and so on.

$$\begin{aligned} P_1 + P_2 &= \sum_{i,j} U_{\alpha i}^* U_{\beta i} U_{\alpha j} U_{\beta j}^* \\ &= \left| \sum_i U_{\alpha i} U_{\beta i}^* \right|^2 \\ &= \delta_{\alpha\beta} \end{aligned}$$

$$\begin{aligned} P_3 &= -2 \sum_{i \neq j} U_{\alpha i}^* U_{\beta i} U_{\alpha j} U_{\beta j}^* \sin^2\left(\frac{L}{4E} \Delta m_{ji}^2\right) \\ &= -2 \sum_{i>j} U_{\alpha i}^* U_{\beta i} U_{\alpha j} U_{\beta j}^* \sin^2\left(\frac{L}{4E} \Delta m_{ij}^2\right) - 2 \sum_{i<j} U_{\alpha i}^* U_{\beta i} U_{\alpha j} U_{\beta j}^* \sin^2\left(\frac{L}{4E} \Delta m_{ji}^2\right) \\ &= -2 \left\{ \sum_{i>j} \sin^2\left(\frac{L}{4E} \Delta m_{ij}^2\right) [U_{\alpha i}^* U_{\beta i} U_{\alpha j} U_{\beta j}^* + (U_{\alpha i}^* U_{\beta i} U_{\alpha j} U_{\beta j}^*)^*] \right\} \\ &= -4 \left\{ \sum_{i>j} \Re(U_{\alpha i}^* U_{\beta i} U_{\alpha j} U_{\beta j}^*) \sin^2\left(\frac{L}{4E} \Delta m_{ij}^2\right) \right\} \end{aligned}$$

Similar to P_3 we can manipulate P_4 and get

$$P_4 = 2 \left\{ \sum_{i>j} \Im(U_{\alpha i}^* U_{\beta i} U_{\alpha j} U_{\beta j}^*) \sin\left(\frac{L}{2E} \Delta m_{ij}^2\right) \right\}$$

The probability equation now reads,

$$\begin{aligned} P(\alpha \rightarrow \beta) &= \delta_{\alpha\beta} - 4 \sum_{i>j} \Re(U_{\alpha i}^* U_{\beta i} U_{\alpha j} U_{\beta j}^*) \sin^2\left(\frac{L}{4E} \Delta m_{ij}^2\right) \\ &\quad + 2 \sum_{i>j} \Im(U_{\alpha i}^* U_{\beta i} U_{\alpha j} U_{\beta j}^*) \sin\left(\frac{L}{2E} \Delta m_{ij}^2\right) \end{aligned} \quad (2.21)$$

Including \hbar and c , we can write the probability such that Δm_{ij}^2 is in eV² L is in km

and E is in GeV.

$$P(\alpha \rightarrow \beta) = \delta_{\alpha\beta} - 4 \sum_{i>j} \Re(U_{\alpha i}^* U_{\beta i} U_{\alpha j} U_{\beta j}^*) \sin^2(1.267 \frac{L}{E} \Delta m_{ij}^2) + 2 \sum_{i>j} \Im(U_{\alpha i}^* U_{\beta i} U_{\alpha j} U_{\beta j}^*) \sin(2.534 \frac{L}{E} \Delta m_{ij}^2) \quad (2.22)$$

With Δm_{ij}^2 defined as $m_i^2 - m_j^2$. For three-flavour, we will have three mixing angles and one phase. The one phase is called CP violating phase. In principle, we can choose any parameterisation. We can define another invariant, the Jarlskog invariant, which quantifies the CP violation[11]. With the parameterisation shown in 2.3,

$$J = c_{12}(c_{13}^2) c_{23} s_{12} s_{13} s_{23} \sin(\delta_{\text{cp}})$$

Using equation 2.21, curves were plotted in fig 2.2. A log scale graph of survival probability for electron-neutrino is also shown for better visualisation

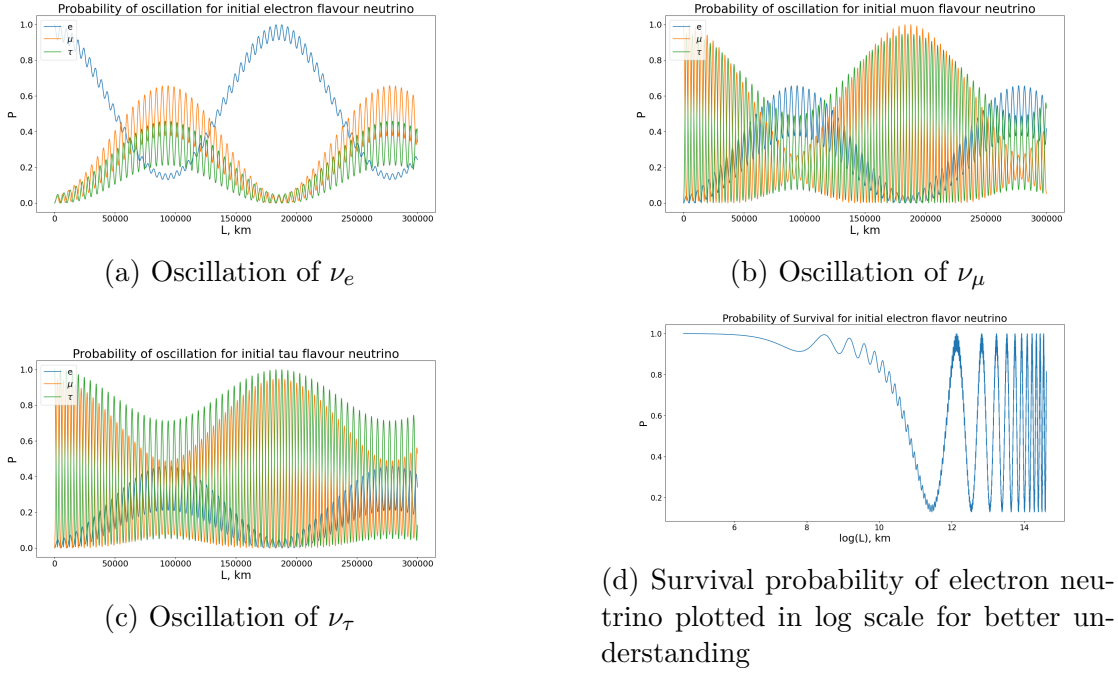


Figure 2.2: Different oscillations of neutrinos

The parameter values⁵ used to plot the oscillation graph shown in 2.2 is listed in table 2.1.

Table 2.1: Parameters

Parameter	best-fit value used
θ_{12}	33.48°
θ_{13}	8.52°
θ_{23}	42.2°
δ_{CP}	-
$ \Delta m_{12}^2 $	$8 \times 10^{-5} \text{ eV}^2$
$ \Delta m_{13}^2 $	$3.08 \times 10^{-3} \text{ eV}^2$
$ \Delta m_{23}^2 $	$3 \times 10^{-3} \text{ eV}^2$

⁵ δ_{CP} parameter was not considered for plotting

2.5 Matter Effect

In the last two sections, we derived the neutrino oscillation in vacuum. If we consider the neutrino propagating through matter, we should modify the Hamiltonian to include the interaction potential that will arise. The matter effect will modify the values of parameterisation significantly[12][13]. This effect is important for far-end detectors. We can neglect matter effect and oscillation probability for near-end detectors, like Minerva, since it is near the neutrino beam.

Considering the matter effect, we can derive probability equations similar to what we did earlier⁶. It is also possible to formulate it to resemble the equation we already derived. But the values of the parameters will be different.

2.6 Neutrino Mass Hierarchy: Inverted and Normal ordering

In deriving neutrino oscillation for three flavour, we have seen three mass-squared differences, Δm_{21}^2 , Δm_{32}^2 and Δm_{31}^2 . Since they should obey $\Delta m_{21}^2 + \Delta m_{32}^2 + \Delta m_{31}^2 = 0$, only two of them are discussed. From experiments[14], it is observed that Δm_{21}^2 is positive definite, therefore m_1 is always less than m_2 . This reduces the hierarchy into two different orderings: $m_3 >> m_2$ (or m_1) or $m_3 << m_1$. The former is known as Normal Ordering(NO), and the latter is called Inverted Ordering(IO).

⁶Appendix B

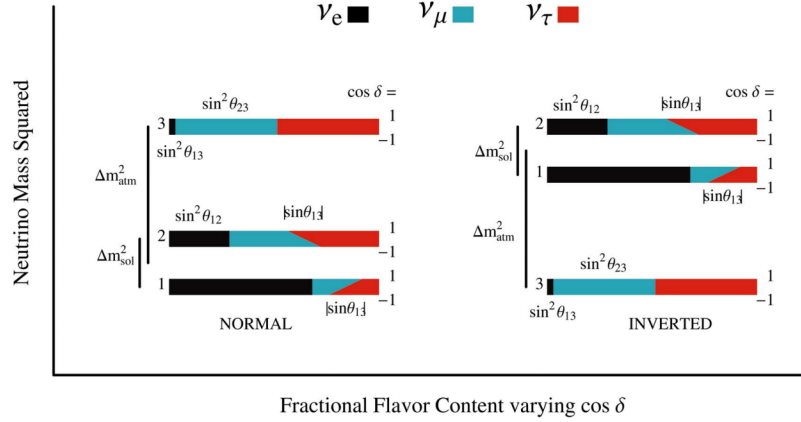


Figure 2.3: Normal Inverted Mass ordering[14]

2.7 Neutrino Interaction

Neutrinos, when interacting with a fermion, can interact via the weak force. These can be Neutral current (involving Z boson) or Charged Current(involving W boson). For example, Muon-neutrino interacting with a neutron giving muon and proton as products, is an example of charged current interaction which has W boson as a propagator. In this interaction, initially, we had two particles (ν_μ and neutron), and the result had two particles (proton and muon). Here, the initial particles is not the same as the end particles. Hence this interaction, 2p-2p, is called quasi-elastic. Therefore $\nu_\mu + n \rightarrow p + \mu^-$ is a Charged-Current Quasi-Elastic (CCQE) interaction.

CCQE: Energy reconstruction

The main aim of this project is to determine the energy of the muon-neutrinos for the interaction $\nu_\mu + n \rightarrow p + \mu^-$. Considering the QE mechanism, the energy for muon-neutrino can be calculated using the formula[15],

$$E_{CC}^\nu = \frac{m_p^2 - m^2 + 2E'(m_n - B) - (m_n - B)^2}{2(m_n - B - E' + k' \cos \theta_\mu)} \quad (2.23)$$

where,

m_p : –Mass of proton.

m : –Mass of muon.

E' : –Energy of muon.

m_n : –Mass of neutron.

B : –Binding energy of neutron inside nucleus⁷.

k' : –Magnitude of momentum of the muon.

θ_μ : –Angle between muon and muon-neutrino direction.

Cross-sections of different interaction are shown in fig 2.4. The RES and DIS in fig 2.4 stands for Resonant Pion Production and Deep Inelastic Scattering. QE is Quasi-Elastic, shown in fig 2.5b.

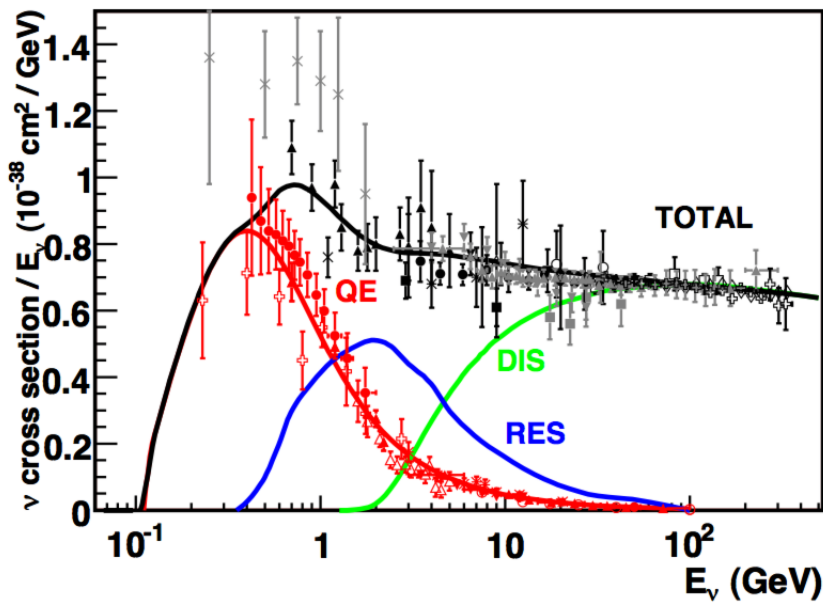
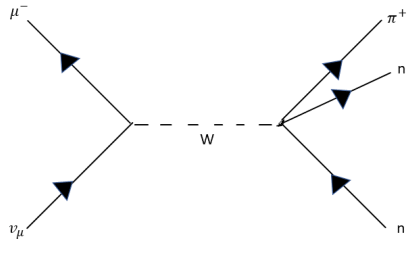
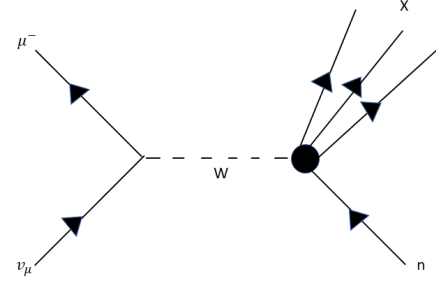


Figure 2.4: Cross section of different interaction of muon-neutrino[16]

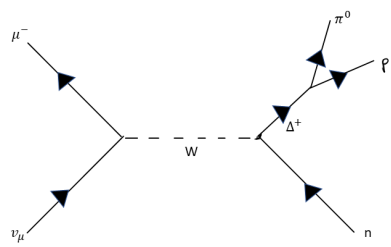
Feynman diagrams for RES, QE, and DIS are shown in fig 2.5



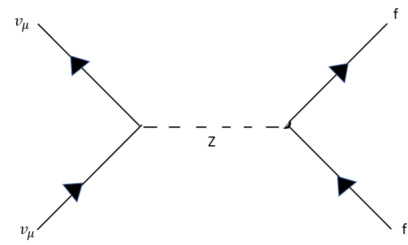
(a) Coherent Pion Production(here n can be neutron or proton)



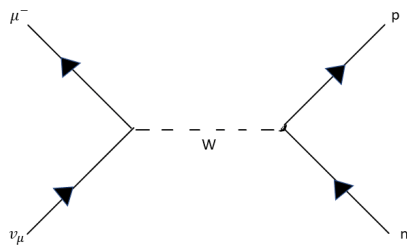
(b) Deep Inelastic Scattering



(c) Resonance: neutral pion production



(d) Neutral current involving Z boson.
f represents a fermion(Elastic collision,
EC)



(e) charged-current interaction involving
W boson(Quasi elastic, QE)

Figure 2.5: Different neutrino interaction. The time axis is vertical in all figures

Flux of Neutrinos

Consider a beam of the muon-neutrino incident on a detector. The event rate is calculated as

$$N_l(E_\nu) = P(\nu_\mu \rightarrow \nu_l)(E_\nu, L)\sigma(E_\nu)\Phi_\nu(E_\nu)\epsilon(E_\nu) \quad (2.24)$$

where,

E_ν :- Energy of the neutrino

L :- Distance travelled by neutrino

$P(\nu_\mu \rightarrow \nu_l)(E_\nu, L)$:- Probability to change to flavor l

$\sigma(E_\nu)$:- Interaction Cross-section

$\Phi_\nu(E_\nu)$:- Neutrino Flux

$\epsilon(E_\nu)$:- Detector Efficiency

In this formula (2.24), the energy appears in all the terms. Therefore, it is important to estimate the energy of neutrinos to find the flux.

Chapter 3

MINERvA

3.1 Introduction

Minerva (Main Injector Experiment νA^1) is a tracking detector which uses a solid-state scintillator tracker. The dimensions of the detector are 3.88 m across, 4.48 m high, and 4.7 m long[17]. The Minerva collaboration was a joint effort between high-energy physicists and nuclear physicists. The neutrino oscillation parameters discussed in Chapter 2 must be measured with high precision. For this, studies related to neutrino collision cross-sections are necessary to remove the uncertainties². Minerva uses muon-neutrino supplies by NuMI beam for the experiment.

The main goal of Minerva is to study the interaction of neutrinos with different nuclei.

¹ ν is neutrino and A denotes mass number

²see appendix C.1

3.2 NuMI

The Protons from Linac pass through the booster and enter the main injector. In Linac, the energy increases to 400 MeV, and the booster accelerates to 8 GeV (fig 3.1).

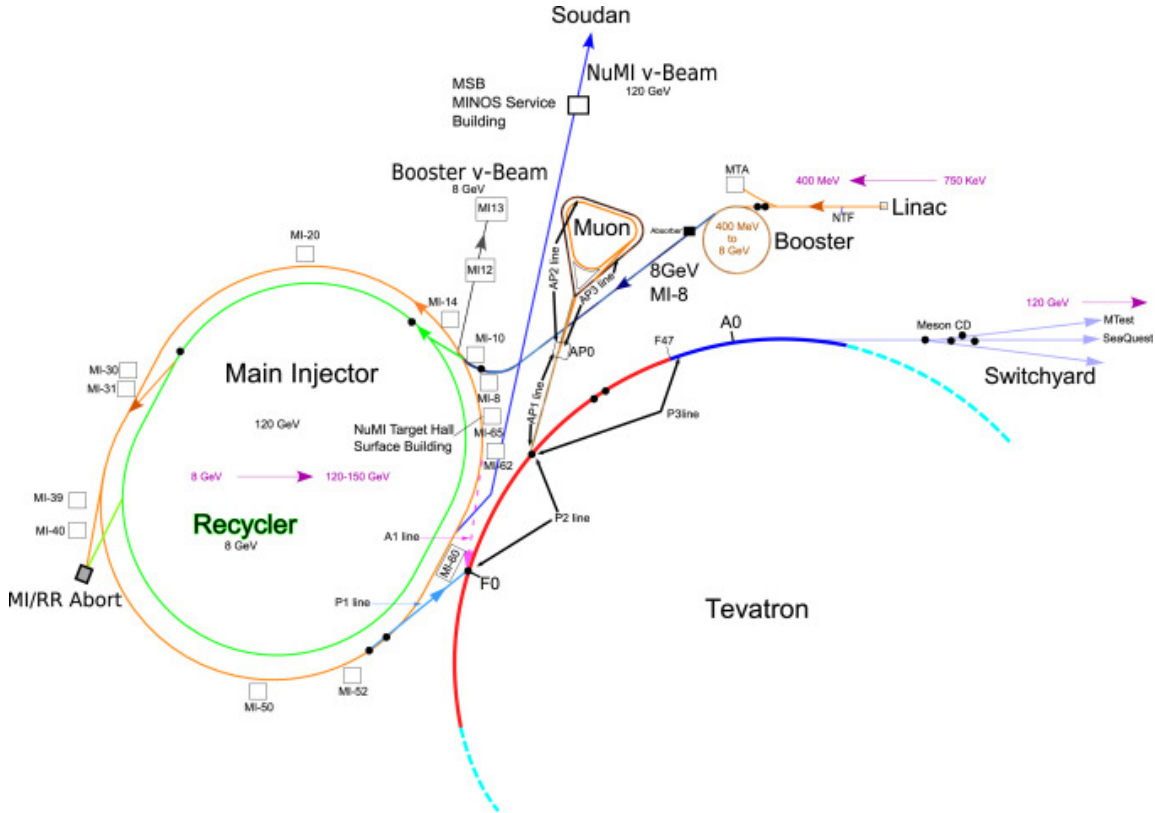


Figure 3.1: Different accelerators[18]

These protons then pass through the main injector and reach 120-160 GeV. The schematic of NuMI is shown in 3.2 The protons are directed to a block of graphite/beryllium target. The proton-graphite collision creates a bunch of pions and Kaons. The beam being antineutrino or neutrino depends on the charge of pion

and Kaon. They can be selected utilising magnetic horns, which can focus positive particles(or negative ones, depending on configuration); in other words, they do not allow negative particles to pass through.

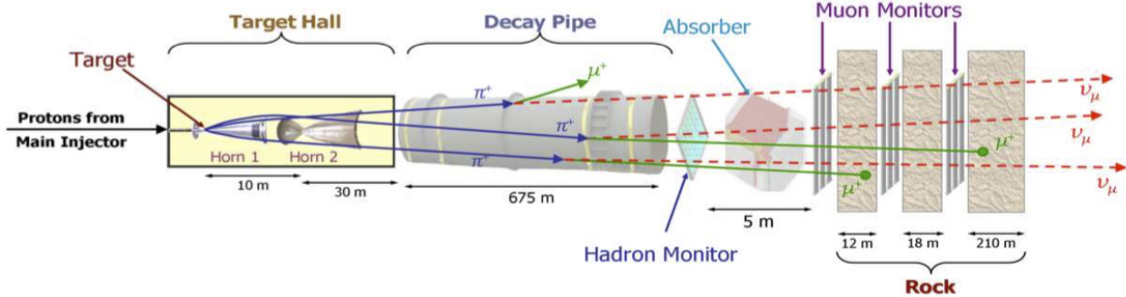


Figure 3.2: NuMI:Neutrino production(neutrino mode)[19]

The κ^+ and π^+ particles decay to give muon-neutrino(κ^- and π^- gives muon-antineutrino) as shown in 3.1.

$$\begin{aligned}\kappa^+ &\rightarrow \mu^+ + \nu_\mu \\ \kappa^+ &\rightarrow \pi^+ + \pi^0 \\ \pi^+ &\rightarrow \mu^+ + \nu_\mu\end{aligned}\tag{3.1}$$

The absorbers and muon-monitors absorb all particles, allowing only neutrinos to pass through. By adjusting the position of the target in NuMI, different energy neutrinos can be produced. Minerva operated in medium energy(peaked at 6 GeV) as well as low energy (peaked at 3 GeV).

3.3 Nuclear Targets and Detector

The Minerva experiment was primarily focused on studying the interaction of (muon) neutrino with different nuclei. The targets in Minerva include Helium(He), Lead (Pb), Carbon (C) and Water (H_2O)(shown in Fig 3.3).

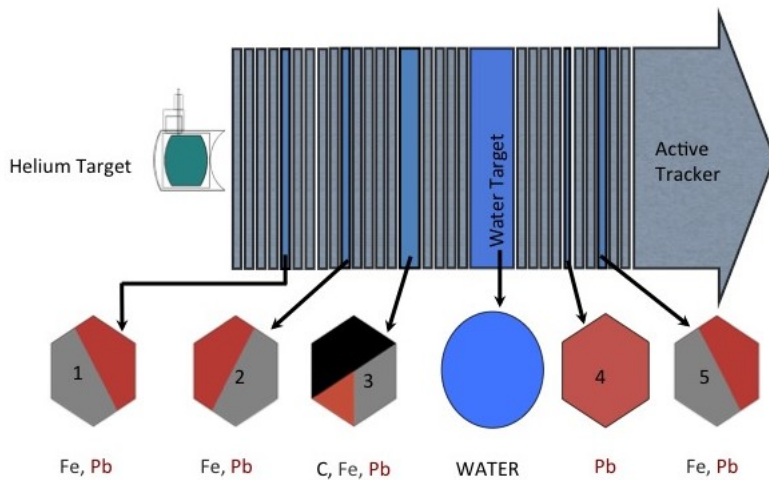


Figure 3.3: Minerva Nuclear targets

The detector or tracker region contains hydrocarbon, principally comprised of carbon. This forms a target medium for neutrino interaction. Hence the tracker region of the detector is active and is called active tracker region.

The tracker region is made of extruded plastic scintillator. The scintillator has a triangular cross-section and is optically coupled to WLS³ fibre. The plastic scintillator is made of polystyrene doped with 1% PPO⁴ and .03% POPOP⁵. The fluorescent

³Wavelength Shifting

⁴2,5-diphenyloxazole

⁵1,4-bis (5-phenyloxazol-2-yl)benzene

dopants emit blue light on de-excitation. The WLS fibre is Y-doped, S, multi-clad provided by Kuraray Corporation. The WLS fibre, as the name says, shifts the wavelength of light emitted from the tracker. The output of WLS will be green light compared to blue emitted by the scintillator. The WLS fibre outputs are fed into PMT.

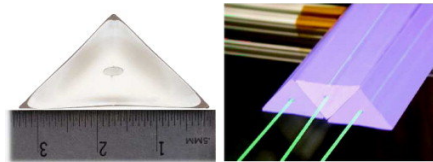


Figure 3.4: Triangular Plastic scintillator[Right], with WLS fibre[Left][20]



Figure 3.5: PMT[20]

The Tracker region consists of arrays of hexagonal planes consisting of long scintillators. Each array plane can be one of three different view planes: X, U and V. The X view is vertical with no deviation. The NuMI beam is assumed along the Z-direction, and the different planes lie in x-y. The U-plane is rotated to 60°clockwise with respect to the X-plane in X-Y, and V-plane is rotated 60°anti-clockwise.

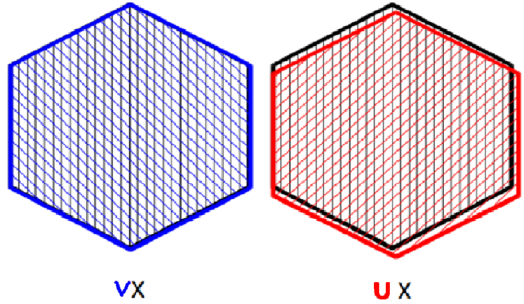


Figure 3.6: X, U and V planes

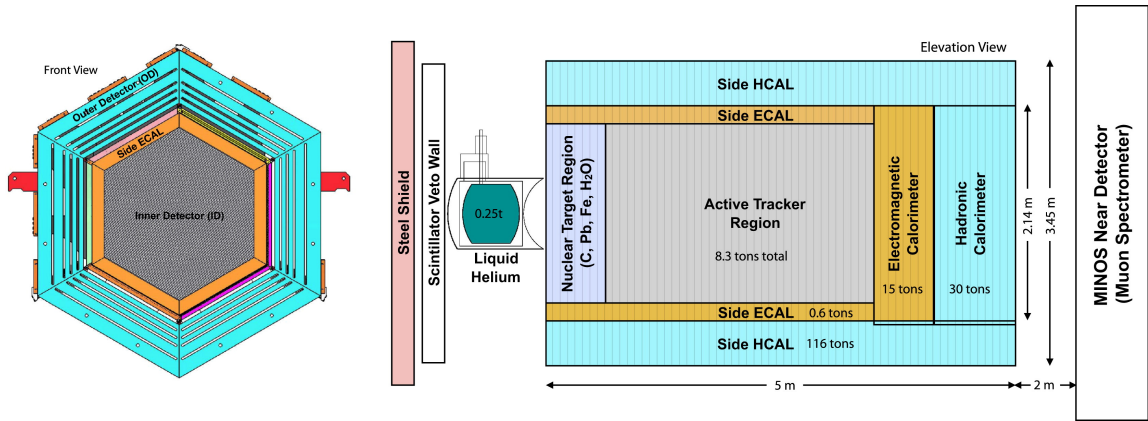


Figure 3.7: Minerva. Right: Cross-sectional view. Left: Longitudinal view showing different components[20]

The veto wall seen in fig 3.7 is used to identify the neutrino interactions that might have happened with nuclei present before the nuclear targets.

3.4 Calorimetry and Minos

3.4.1 Calorimetry

The Minerva detector has an electromagnetic and a hadronic calorimeter to measure the energy of the particle and identify them. The electromagnetic calorimeter(ECAL) is on the inner side, and the hadronic calorimeter(HCAL) is on the outer side. HCAL relies on hadronic showers involving strong force(for instance, inelastic and elastic collisions with nuclei lead to showers)[21]. ECAL is designed to measure the total energy of particle like electrons and photons(which interact electromagnetically) by total absorption.

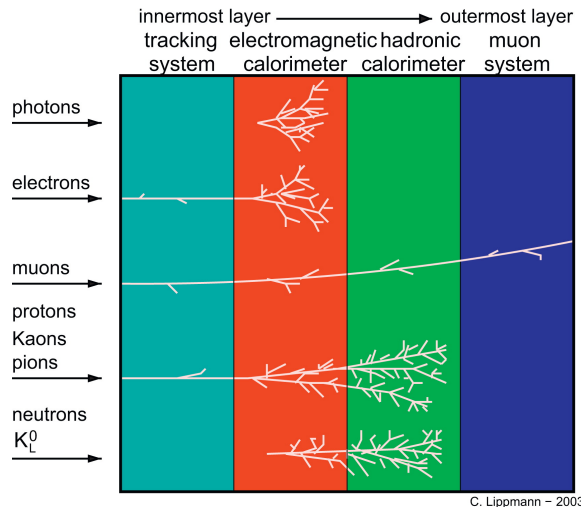


Figure 3.8: Differential identification of particles[22]

The arrangement of the calorimeters and trackers as in fig 3.7 allows identification of different particles as shown in fig 3.8.

HCAL is bigger in volume than ECAL because the particles that lose energy in ECAL

do at a higher rate than those that lose energy in HCAL. For example, in lead for a good electromagnetic shower, we need a depth of 14cm, while for a good hadronic shower, we require 171 cm [23]. It is also for this reason that HCAL is placed behind ECAL.

3.4.2 Minos

MINOS is another near(and far) detector. The Minerva detector lies directly before the MINOS near detector and uses the NuMI beam priorly intended to run MINOS. The particles which escape Minerva volume would enter MINOS. If that happens, the particle's energy can be evaluated and collected as data. The particles detected in MINOS are backtracked to verify that they came from the Minerva volume.

3.5 Resolution

From simulations, energy resolutions and other important characteristics were found and reported in literature[20][17]. The position resolution of the detector is reported to be 3mm. The Calorimetric energy resolution is reported by Aliaga et al [20] is $\frac{\sigma}{E} = 0.134 \oplus \frac{0.290}{\sqrt{E(GeV)}}$. The Birks law constant is also constrained to be 0.133 ± 0.040 mm/MeV. The average (calorimetric) energy resolution reported by Howard Budd [17] is $\frac{\Delta E}{E} = \frac{23\%}{\sqrt{E(GeV)}}$. This considers that all the hadronic showers lie within the detector. The energy resolution has an energy dependence shown as $\frac{\Delta E}{E} = 4\% + \frac{18\%}{\sqrt{E(GeV)}}$. The momentum resolution($\frac{\Delta p}{p}$) for muons that stopped within the Minerva is reported to be 5%, and for muons that enter minos is 13%. For quasi-elastic events, the RMS vertex uncertainties are 9mm and 12mm for transverse and

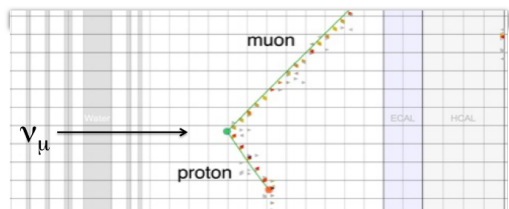
parallel directions with the beam, respectively. The simulations run by them showed an impact parameter of 2 mm and an angular resolution of (less than) 9 mrad.

3.6 Arachne

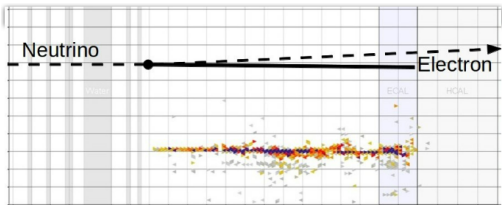
The Minerva collected a vast amount of data from March 2010 to February 2019. The data acquired from the Minerva experiment is available for visualisation and collection via an Arachne website[24]. The event display is sliced in different time intervals. Each slice gives the energy loss in the detector, and the path can be reconstructed accordingly. The interface also provides the utility to select a track and copy necessary data such as momentum 3-components, velocity and kinetic energy. The interface also shows track length and direction. The display shows the energy detected along with the reconstructed track. This enables the user to handpick the interaction of interest. Comprehensive handpicking is one of the features Minerva-Arachne offers.

3.6.1 Arachne-display

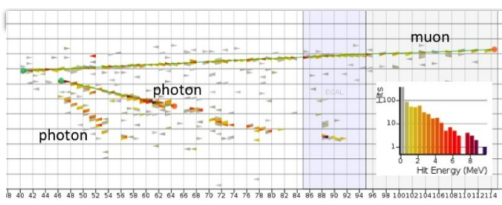
The detected tracks are displayed in a panel. In this panel, one could interpret the possible interaction that could have happened and use reasoning to collect the desired data. Fig 3.9 shows a few interactions Minerva “saw”.



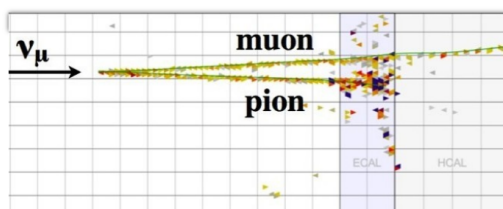
(a) Pure CCQE interaction[25]



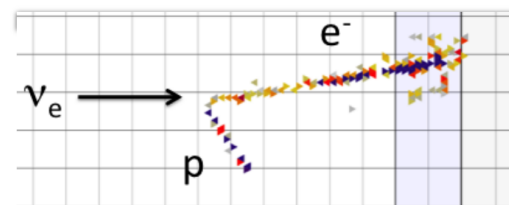
(c) Neutrino-electron elastic scattering[27]



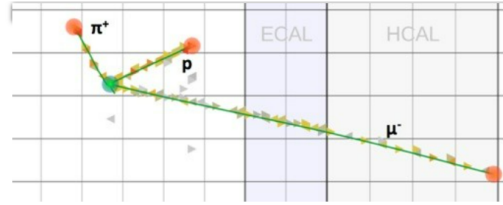
(e) Single neutral pion production by charged-current[29]



(b) coherent charged pion production[26]



(d) Electron Neutrino Quasielastic Scattering[28]



(f) Charged pion production via charged-current[30]

Figure 3.9: Minerva event display samples(All images taken from Minerva Website)

Chapter 4

Results and Discussions

Data and Analysis

The data is hand scanned for CCQE and collected from the Minerva Arachne website. The nucleus where interaction happens lies in the active tracker and is assumed to be carbon-12. The POT¹ of NuMI corresponding to medium energy configuration was reported to be 12.4×10^{20} [31]. Of these interactions, only .8 million were reported to be CCQE interactions. This study uses data from only 1951 interactions. The criteria looked for in samples were,

1. **A Short track** which is usually proton track.
2. **A Long track** which is usually Muon track.
3. **A common vertex** for the short and long track.

¹Proton on target

- No other track should be present in the vertex.

The root-framework[32] developed by CERN is used for data analysis.

From the data collected, the energy and momentum of neutrinos are calculated.

4.1 Momentum

4.1.1 Muon - Momentum

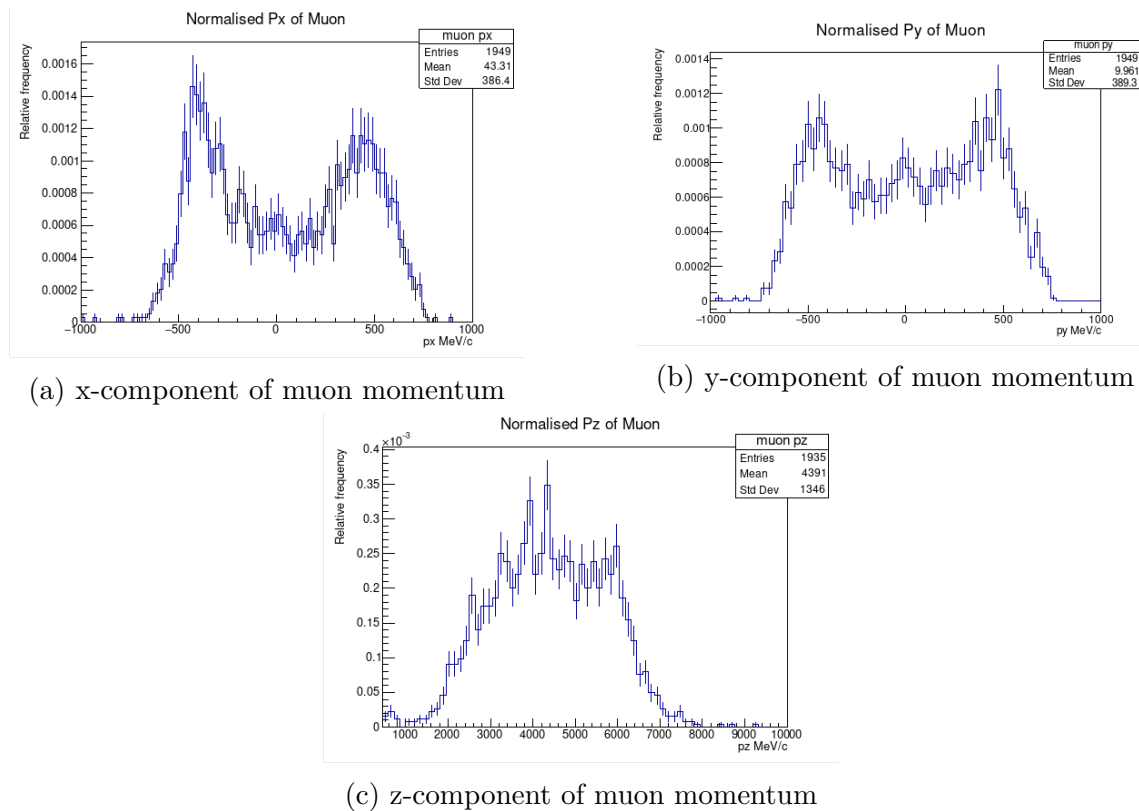


Figure 4.1: Distribution of Muon momentum. All plots are integral normalised.

4.1.2 proton - Momentum

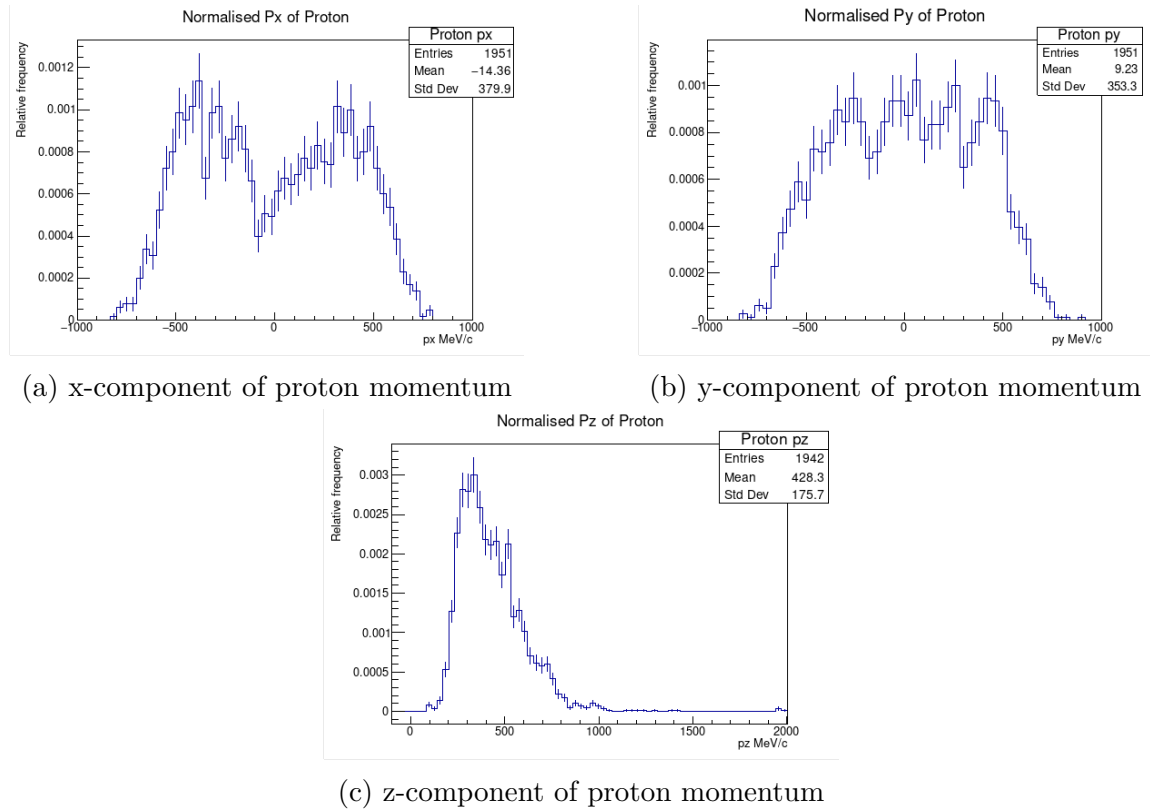


Figure 4.2: Distribution of proton momentum. All plots are integral normalised.

4.1.3 Muon-neutrino - Momentum

The neutron is assumed to be in rest initially. Under this assumption, we can find momentum of muon-neutrino by conservation of linear momentum. The momentum of the muon-neutrino is simply the sum of momentum of proton and muon.

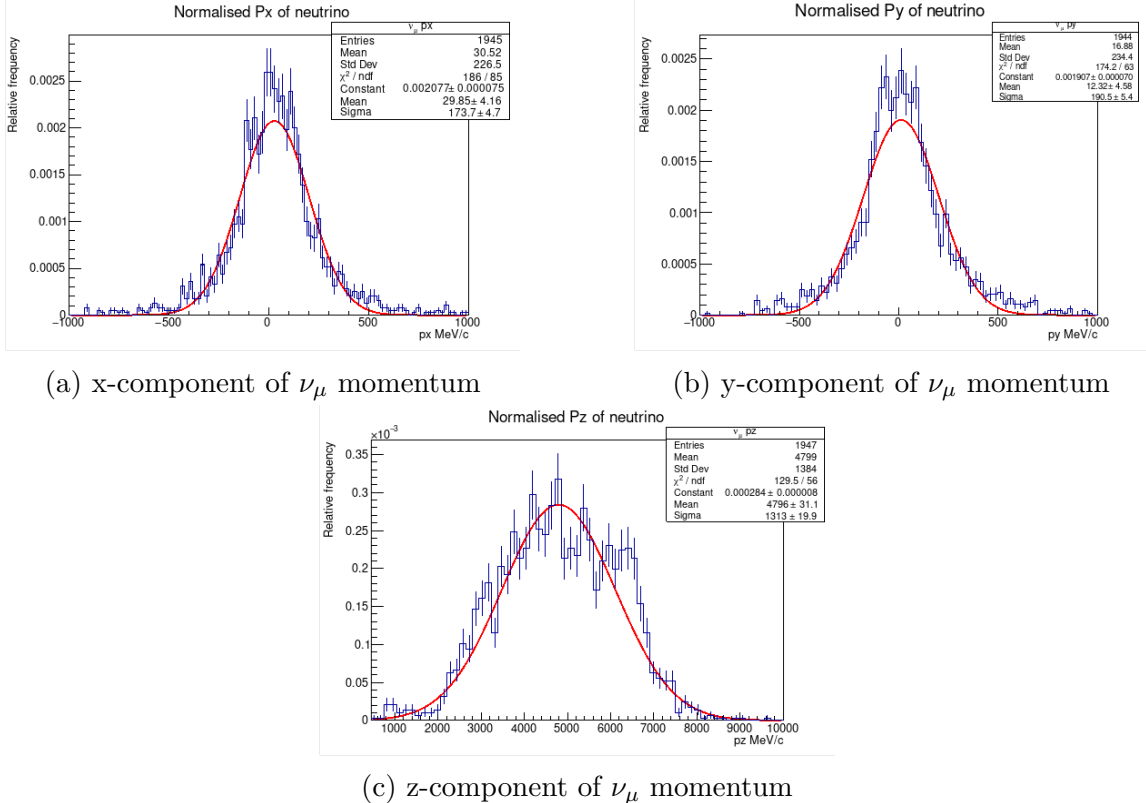


Figure 4.3: Distribution of ν_μ momentum. All plots are integral normalised.

Here, we can see that the x and y components are distributed around zero, while the z component is not. This agrees that the neutrino beam is aligned along the z-axis.

From the plots of P_x and P_y of ν_μ momentum, we can calculate the uncertainty in position.

For P_x :

From graph 4.3a, the standard deviation of fitted gaussian curve = 173.7 MeV/c

$$\text{FWHM}^2 = 2.355 \times \text{standard deviation} = 2.355 \times 173.7 = 409.0635 \text{ MeV}/c$$

²Full width at half maximum

Uncertainty, $\Delta P_x = \frac{FWHM}{2} = \frac{409.0635}{2} \text{ MeV/c}$

³Uncertainty in position x, $\Delta X = \frac{\hbar}{2 \times \Delta P_x} = 0.488922 \text{ fm}$

For P_y :

From graph 4.3b, the standard deviation of fitted gaussian curve = 190.5 MeV/c

FWHM = $2.355 \times$ standard deviation = $2.355 \times 190.5 \text{ MeV/c} = 448.6275 \text{ MeV/c}$

Uncertainty, $\Delta P_y = \frac{FWHM}{2} = \frac{448.6275}{2} \text{ MeV/c}$

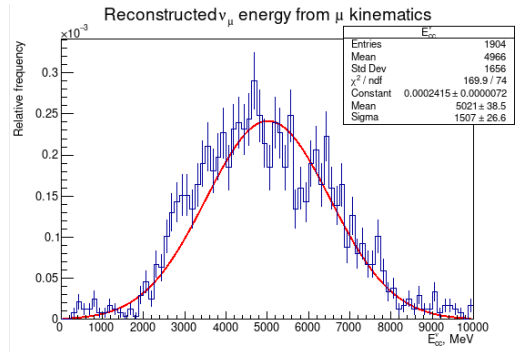
Uncertainty in position y, $\Delta Y = \frac{\hbar}{2 \times \Delta P_y} = 0.4458 \text{ fm}$

For carbon-12 nucleus, radius = 2.7 fm.

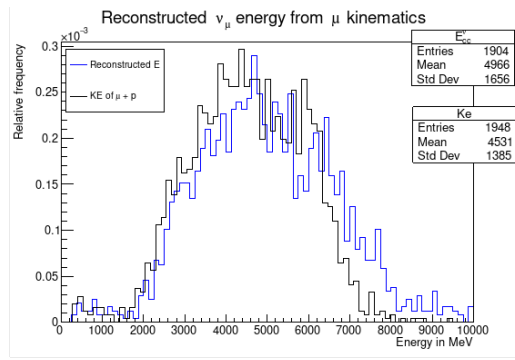
4.2 Reconstructed Energy

Equation 2.23 is used to find the energy of the muon-neutrino. A histogram showing the distribution is plotted and fitted with a Gaussian curve. Another histogram of the sum of muon and proton kinetic energies is also compared.

³Taking $\hbar c = 200 \text{ MeV} \cdot \text{fm}$



(a) Reconstructed Energy



(b) Comparing reconstructed energy with the sum of kinetic energies of μ and proton

Figure 4.4: Reconstructed Energy of ν_μ by (a) QE energy reconstruction; (b) sum of kinetic energies of products

4.3 de Broglie wavelength

From the neutrino momentum, it is possible to calculate the de Broglie wavelength. A plot is shown in fig 4.5, where the magnitude of momentum is used to calculate the wavelength.

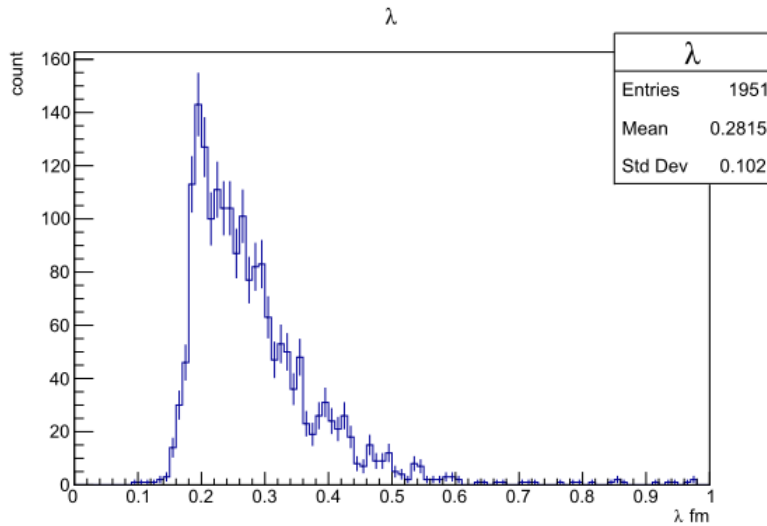


Figure 4.5: de Broglie wavelength of μ -neutrinos($1 \text{ fm} = 10^{-15} \text{ m}$)

From the fig 4.5, it is evident that all ν_μ has wavelength below 1 fm, most of which lie between 0.2 to 0.3 fm. The radius of a proton can be approximated as 0.8 fm[33]. It is safe to conclude that the neutrinos are interacting at the nucleon level and can “see” inside the nucleus.

4.4 Caveats in analysis

The source of errors in the data analysis is from data collection interpreting the visual interface. The analysis is based on the CCQE interaction of muon-neutrino. However, some interactions mimic CCQE and other kinds, which is CCQE, but due to FSI⁴, it doesn’t appear as CCQE. We do not incur errors from the latter, only leading to a loss in data, but the former one will induce errors in our calculation. The

⁴Final State Interaction

interaction could lead to intermediate Δ particle productions(also gives a muon like in CCQE) in the nucleus, which can decay into neutral pion and proton 2.5c. The tracker medium cannot track the neutral particle, but we will see muon and proton track. The kinematics of pion will be lost, and treating it as CCQE will induce errors in analysis. From fig 2.4, we can see the resonant pion production has equal chances as QE to happen at the chosen energy of the neutrino. Another interaction, shown in fig 2.5a, also induces error. We would see a pion and muon track similar to CCQE and use the wrong formula. Also, if the interacting particle is proton(instead of neutron in 2.5a), and if another nucleus absorbs the pion, we will incur energy estimation errors. This is one possible explanation for the second significant peak in figure 4.4.

Chapter 5

Conclusion

A sample of 1951 interactions was collected and analysed. Plots for three components of momentum of muon and neutron were plotted for visualisation. From the kinematics of muon, the Energy of muon-neutrino were calculated and plotted. The Gaussian fit of the plot curve showed mean was at 5.021 GeV with a standard deviation of 1.507 GeV. From the momentum of neutrino de Broglie wavelength was calculated, which showed a mean at 0.28 fm.

Appendices

Appendix A

Dirac Equation

A.1 Dirac Equation

The Dirac equation is

$$(\iota\gamma^\mu\partial_\mu - m)\psi(\vec{x}, t) = 0 \quad (\text{A.1})$$

Using Feynman slash notation, the equation can be re-written as,

$$(i\cancel{\partial} - m)\psi(x) = 0 \quad (\text{A.2})$$

For spin-half free particle,

$$\psi(\vec{x}, t) = N u(\vec{p}) e^{-\iota p^\mu x_\mu}; p^\mu = (E, \vec{p}) \quad (\text{A.3})$$

The $u(\vec{p})$ will satisfy the equation,

$$(\not{p} - m)u(\vec{p}) = 0 \quad (\text{A.4})$$

If we consider the case $p = 0$, then,

$$(E\gamma^0 - m)u(\vec{p}) = 0 \text{ with } u(\vec{p}) = \begin{pmatrix} u_1 \\ u_2 \\ u_3 \\ u_4 \end{pmatrix} \quad (\text{A.5})$$

We can find solutions by requiring the $\det(E\gamma^0 - mI)$ to be zero. This gives us four eigenvectors:

$$u_1 = \begin{pmatrix} 1 \\ 0 \\ 0 \\ 0 \end{pmatrix}; u_2 = \begin{pmatrix} 0 \\ 1 \\ 0 \\ 0 \end{pmatrix}; u_3 = \begin{pmatrix} 0 \\ 0 \\ 1 \\ 0 \end{pmatrix}; u_4 = \begin{pmatrix} 0 \\ 0 \\ 0 \\ 1 \end{pmatrix} \quad (\text{A.6})$$

u_1 and u_2 has Energy $E = m$, and u_3 and u_4 has $E = -m$. The states of Dirac solutions are called spinor because they explain spin of the particle.

A.2 Weyl equation

For a general case, $p \neq 0$, the 4-component $u(\vec{p})$ is expressed in terms of two 2-component spinors, u_a and u_b .

$$u(\vec{p}) = \begin{pmatrix} u_a(\vec{p}) \\ u_b(\vec{p}) \end{pmatrix}; u_a(\vec{p}) = \begin{pmatrix} u_1 \\ u_2 \end{pmatrix}; u_b(\vec{p}) = \begin{pmatrix} u_3 \\ u_4 \end{pmatrix} \quad (\text{A.7})$$

Solving dirac equation with this spinors will also give us positive and negative solutions for energy. The relations for positive energy satisfied by the spinors can be obtained as

$$(p^0 - m)u_a(\vec{p}) - (\vec{\sigma} \cdot \vec{p})u_b(\vec{p}) = 0 \quad (\text{A.8})$$

$$(\vec{\sigma} \cdot \vec{p})u_b(\vec{p}) - (p^0 - m)u_a(\vec{p}) = 0 \quad (\text{A.9})$$

Rearranging the above equation and adding and subtracting gives

$$(p^0 - \vec{\sigma} \cdot \vec{p})(u_a(\vec{p}) + u_b(\vec{p})) = m(u_a(\vec{p}) - u_b(\vec{p})) \quad (\text{A.10})$$

$$(p^0 + \vec{\sigma} \cdot \vec{p})(u_a(\vec{p}) - u_b(\vec{p})) = m(u_a(\vec{p}) + u_b(\vec{p})) \quad (\text{A.11})$$

Defining,

$$u_L(\vec{p}) = \frac{(u_a(\vec{p}) - u_b(\vec{p}))}{2} \quad (\text{A.12})$$

$$u_R(\vec{p}) = \frac{(u_a(\vec{p}) + u_b(\vec{p}))}{2} \quad (\text{A.13})$$

Substituting in eqn A.10,

$$(p^0 - \vec{\sigma} \cdot \vec{p}) u_R(\vec{p}) = m u_L(\vec{p}) \quad (\text{A.14})$$

$$(p^0 + \vec{\sigma} \cdot \vec{p}) u_L(\vec{p}) = m u_R(\vec{p}) \quad (\text{A.15})$$

These two equations are coupled by the mass term m . If we consider mass-less particles, i.e., $m = 0$, then,

$$p^0 u_R(\vec{p}) = \vec{\sigma} \cdot \vec{p} u_R(\vec{p}) \quad (\text{A.16})$$

$$p^0 u_L(\vec{p}) = -\vec{\sigma} \cdot \vec{p} u_L(\vec{p}) \quad (\text{A.17})$$

These equations are called Weyl equations[5]. They are not invariant under parity transformation.

Appendix B

Matter Effect

Neutrinos travelling in matter can undergo forward scattering with specific particles depending on their flavour. This gives a potential involving interaction energy in the Hamiltonian. There are two ways this can happen:

1. ν_α can interact with charged lepton l_α (where α is flavor) by exchanging a W boson. The matter around is rich mostly in electrons. Hence this interaction is significant only for ν_e . This interaction is Charged-current. The interaction potential is proportional to electron number density in the medium and Fermi coupling constant, G_F .

$$V_W = \begin{cases} +\sqrt{2}G_F N_e & \text{for } \nu_e \\ -\sqrt{2}G_F N_e & \text{for } \bar{\nu}_e \\ 0 & \text{all other } \nu \end{cases}$$

2. All neutrinos can interact with suitable electron, proton and neutron by ex-

changing Z boson. Since protons and electron are opposite in charge and equal in magnitude, we can cancel them. This interaction is flavour independent, and the potential V_Z depends on the neutron number density.

$$V_Z = \begin{cases} -\frac{1}{2}\sqrt{2}G_F N_n & \text{for } \nu \\ +\frac{1}{2}\sqrt{2}G_F N_n & \text{for } \bar{\nu} \end{cases}$$

The next few sections discuss the matter effect for two-flavour oscillation.

B.1 Hamiltonian for neutrino in vacuum

The time-independent Schrödinger equation for a neutrino travelling through a vacuum is, taking $c = \hbar = 1$,

$$\iota \frac{\partial}{\partial t} |\nu(t)\rangle = H |\nu(t)\rangle \quad (\text{B.1})$$

If we consider two flavours, e and μ ,

$$|\nu(t)\rangle = \begin{pmatrix} \nu_e(t) \\ \nu_\mu(t) \end{pmatrix} \quad (\text{B.2})$$

$$\begin{aligned} \langle \nu_\alpha | H_{vacuum} | \nu_\beta \rangle &= \langle \sum_i U_{\alpha i} \nu_i | H_{vacuum} | \sum_j U_{\beta j} \nu_j \rangle \\ &= \sum_i U_{\alpha i}^* \langle \nu_i | H_{vacuum} | \nu_i \rangle U_{\beta i} \end{aligned} \quad (\text{B.3})$$

Using the same parametrisation used in equation 2.9, we can find matrix form as,

$$\begin{aligned}\langle \nu_\alpha | H_{vacuum} | \nu_\beta \rangle &= \begin{pmatrix} \cos \theta & -\sin \theta \\ \sin \theta & \cos \theta \end{pmatrix} \begin{pmatrix} E_1 & 0 \\ 0 & E_2 \end{pmatrix} \begin{pmatrix} \cos \theta & \sin \theta \\ -\sin \theta & \cos \theta \end{pmatrix} \\ &= \begin{pmatrix} E_1 \cos^2 \theta + E_2 \sin^2 \theta & E_1 \sin \theta \cos \theta - E_2 \sin \theta \cos \theta \\ -E_1 \sin \theta \cos \theta + E_2 \sin \theta \cos \theta & E_2 \cos^2 \theta - E_1 \sin^2 \theta \end{pmatrix}\end{aligned}\tag{B.4}$$

Using the energy-momentum formula for E_1 and E_2 and using high relativistic approximation $E = p + \frac{m^2}{2p}$, where $p = |\vec{p}|$. Simplifying for each element,

$$\begin{aligned}E_1 \cos^2 \theta + E_2 \sin^2 \theta &= \left(p + \frac{m_1^2}{2p}\right) \cos^2 \theta + \left(p + \frac{m_2^2}{2p}\right) \sin^2 \theta \\ &= -\frac{\Delta m^2}{4p} \cos 2\theta + \frac{m_1^2 + m_2^2}{4p} + p \text{ with } \Delta m^2 = m_2^2 - m_1^2\end{aligned}\tag{B.5}$$

Similarly,

$$\begin{aligned}E_2 \cos^2 \theta + E_1 \sin^2 \theta &= \left(p + \frac{m_2^2}{2p}\right) \cos^2 \theta + \left(p + \frac{m_1^2}{2p}\right) \sin^2 \theta \\ &= \frac{\Delta m^2}{4p} \cos 2\theta + \frac{m_1^2 + m_2^2}{4p} + p \text{ with } \Delta m^2 = m_2^2 - m_1^2\end{aligned}\tag{B.6}$$

$$\begin{aligned}-E_1 \sin \theta \cos \theta + E_2 \sin \theta \cos \theta &= \sin \theta \cos \theta (E_2 - E_1) \\ &= \sin \theta \cos \theta \left(p + \frac{m_2^2}{2p} - \left(p + \frac{m_1^2}{2p}\right)\right) \\ &= \sin 2\theta \left(\frac{\Delta m^2}{4p}\right)\end{aligned}\tag{B.7}$$

Therefore, the vacuum Hamiltonian is, ($E \approx p$),

$$H_{vacuum} \approx \frac{\Delta m^2}{4E} \begin{pmatrix} -\cos 2\theta & \sin 2\theta \\ \sin 2\theta & \cos 2\theta \end{pmatrix} \quad (\text{B.8})$$

In the eqn, we have neglected the diagonal matrix since only the relative phase is important.

B.2 Matter Hamiltonian

The Hamiltonian in matter can be taken as the sum of vacuum-hamiltonian and the interaction potential due to NC (V_Z) and CC (V_W).

$$H_M = H_{vacuum} + V_W \begin{pmatrix} 1 & 0 \\ 0 & 0 \end{pmatrix} + V_Z \begin{pmatrix} 1 & 0 \\ 0 & 1 \end{pmatrix} \quad (\text{B.9})$$

$$= H_{vacuum} + \frac{1}{2}V_W \begin{pmatrix} 1 & 0 \\ 0 & -1 \end{pmatrix} + \left(\frac{V_W}{2} + V_Z\right) \begin{pmatrix} 1 & 0 \\ 0 & 1 \end{pmatrix} \quad (\text{B.10})$$

Ignoring the last term we get,

$$H_M = H_{vacuum} + \frac{1}{2}V_W \begin{pmatrix} 1 & 0 \\ 0 & -1 \end{pmatrix} = H_{vacuum} + \frac{1}{2}\sqrt{2}G_F N_e \begin{pmatrix} 1 & 0 \\ 0 & -1 \end{pmatrix} \quad (\text{B.11})$$

If we define, $x = \frac{2\sqrt{2}G_F N_e E}{\Delta m^2}$, then

$$H_M = \frac{\Delta m^2}{4E} \begin{pmatrix} -(\cos 2\theta - x) & \sin 2\theta \\ \sin 2\theta & (\cos 2\theta - x) \end{pmatrix} \quad (\text{B.12})$$

We can define two variables Δm_M^2 and θ_M , such that

$$\sin^2 2\theta_M = \frac{\sin^2 2\theta}{\sin^2 2\theta + (\cos 2\theta - x)^2} \quad (\text{B.13})$$

$$\Delta m_M^2 = \Delta m^2 \sqrt{\sin^2 2\theta + (\cos 2\theta - x)^2} \quad (\text{B.14})$$

$$m_{1M}^2 = -\frac{1}{2}\Delta m^2 \sqrt{\sin^2 2\theta + (\cos 2\theta - x)^2} \quad (\text{B.15})$$

$$m_{2M}^2 = \frac{1}{2}\Delta m^2 \sqrt{\sin^2 2\theta + (\cos 2\theta - x)^2} \quad (\text{B.16})$$

Probability of Oscillation in Matter: Two Flavor

Using the Hamiltonian, we can find oscillation probability as in Section 2.3. The equation 2.19 will be modified as,

$$P(\nu_e \rightarrow \nu_\mu) = \sin^2 2\theta_M \sin^2(1.267\Delta m_M^2 \frac{L}{E}) \quad (\text{B.17})$$

Appendix C

Additional Context

C.1 Systematic errors

The equation 2.24 shows three terms (apart from the probability of oscillation). These terms has their own errors,

1. **Neutrino Flux:** Not well modelled by MC simulations. Leads to uncertainty regarding hadron production in the source. It also involves uncertainty in focussing and alignments.
2. **Neutrino Interaction Systematics:** Absolute Cross-sectional measurements are needed.
3. **Detector Response:** Sum of errors in calibration, proper coupling of detector parts and other electronic errors.

Minerva was aimed to reduce errors in neutrino interactions. It has analysed neutrino interactions with lead, carbon and water (oxygen) molecules[34][35].

C.2 ROOT

Root is a data analysing framework developed by cern to analyse and plot large amounts of data. The Arachne website also uses root based program in the backend. Root is written in C++. The macros, short program files written to perform a few functions, are written in C++. Root also has support for Python and jupyter notebook.

Bibliography

- [1] W. Haxton, Annual Review of Astronomy and Astrophysics **33**, 459 (1995).
- [2] R. Davis Jr et al., Physical Review Letters **20**, 1205 (1968).
- [3] J. N. Bahcall et al., Physical Review Letters **20**, 1209 (1968).
- [4] V. Gribov et al., Physics Letters B **28**, 493 (1969).
- [5] W. Hermann, Zeitschrift für Physik **56**, 330 (1929).
- [6] P. A. M. Dirac, Proceedings of the Royal Society of London. Series A, Containing Papers of a Mathematical and Physical Character **117**, 610 (1928).
- [7] E. Majorana, Il Nuovo Cimento (1924-1942) **14**, 171 (1937).
- [8] M. S. Athar et al., *The physics of neutrino interactions* (Cambridge University Press, 2020).
- [9] J. W. Valle, in Journal of physics: conference series, Vol. 53, 1 (IOP Publishing, 2006), p. 473.
- [10] D. Kruppke, “On theories of neutrino oscillations”, PhD thesis (Diploma Thesis, 2007).
- [11] C. Jarlskog, Physical Review Letters **55**, 1039 (1985).

- [12] L. Wolfenstein, Physical Review D **17**, 2369 (1978).
- [13] S. Mikheyev et al., Il Nuovo Cimento C **9**, 17 (1986).
- [14] O. Mena et al., Physical Review D **69**, 117301 (2004).
- [15] O. Benhar et al., Physical Review D **80**, 073003 (2009).
- [16] J. Hewett et al., arXiv preprint arXiv:1205.2671 (2012).
- [17] H. Budd, International Journal of Modern Physics A **20**, 3073 (2005).
- [18] P. Adamson et al., Nuclear Instruments and Methods in Physics Research Section A: Accelerators, Spectrometers, Detectors and Associated Equipment **806**, 279 (2016).
- [19] A. Blake et al., Nuclear Instruments and Methods in Physics Research. Section A: Accelerators, Spectrometers, Detectors and Associated Equipment **806**, 279 (2016).
- [20] L. Aliaga et al., Nuclear Instruments and Methods in Physics Research Section A: Accelerators, Spectrometers, Detectors and Associated Equipment **743**, 130 (2014).
- [21] P. D. Group et al., Progress of theoretical and experimental physics **2022**, 083C01 (2022).
- [22] C. Lippmann, Nuclear Instruments and Methods in Physics Research Section A: Accelerators, Spectrometers, Detectors and Associated Equipment **666**, 148 (2012).
- [23] D. Barney, Journal of Instrumentation **15**, C07018 (2020).

- [24] N. Tagg et al., Nuclear Instruments and Methods in Physics Research Section A: Accelerators, Spectrometers, Detectors and Associated Equipment **676**, 44 (2012).
- [25] T. Walton et al., Physical Review D **91**, 071301 (2015).
- [26] A. Higuera et al., Physical review letters **113**, 261802 (2014).
- [27] J. Park et al., Physical Review D **93**, 112007 (2016).
- [28] J. Wolcott et al., Physical review letters **116**, 081802 (2016).
- [29] T. Le et al., Physics Letters B **749**, 130 (2015).
- [30] B. Eberly et al., Physical Review D **92**, 092008 (2015).
- [31] X.-G. Lu et al., The European Physical Journal Special Topics **230**, 4243 (2021).
- [32] R. Brun et al., *Root-project/root: v6.18/02*, version v6-18-02, Aug. 2019.
- [33] B. Povh et al., Particles and Nuclei: An Introduction to the Physical Concepts, 75 (2015).
- [34] J. G. Morfin et al., Nuclear Physics B-Proceedings Supplements **149**, 215 (2005).
- [35] D. A. Harris, *Minerva results and prospects*, tech. rep. (Fermi National Accelerator Lab.(FNAL), Batavia, IL (United States), 2022).